Article

Not peer-reviewed version

Effect of Gadolinium-Doped Ceria (GDC) Promoter on the Catalytic Activity of Ni/Al_2O_3 in Methane Dry Reforming

Y. Li , S. B. Nourani Najafi * , P. V. Aravind , A. Mokhov

Posted Date: 26 February 2026

doi: 10.20944/preprints202602.1593.v1

Keywords: Dry reforming of methane;Ni catalysts;Al2O3 support;GDC promoter

 doi:10.20944/preprints202602.1593.v1

Article

Effect of Gadolinium-Doped Ceria (GDC) Promoter on the Catalytic Activity of Ni/Al_2O_3 in Methane Dry Reforming

Y. Li, S.B. Nourani Najafi *, P.V. Aravind and A.V. Mokhov

Energy Conversion, Energy and Sustainability Research Institute Groningen (ESRIG), University of Groningen, The Netherlands

* Correspondence: s.b.nourani.najafi@rug.nl

Abstract

Dry reforming of methane (DRM) is an attractive route for H_2 production and simultaneous CO_2 utilization, but its practical implementation is limited by catalyst deactivation. This study experimentally investigates the catalytic performance of Ni/Al_2O_3 and Gd-doped ceria–promoted $Ni/GDC–Al_2O_3$ catalysts for DRM in a fixed-bed quartz reactor over 400–800 °C at gas residence times of 0.1 s and 0.4 s. Increasing temperature and residence time enhanced CH_4 and CO_2 conversion as well as H_2 and CO yields for both catalysts. The GDC-promoted catalyst exhibited markedly improved activity, achieving conversions and product yields at 0.1 s comparable to those of Ni/Al_2O_3 at 0.4 s and reaching complete CH_4 conversion at about 650 °C, approximately 100 °C lower than the Ni/Al_2O_3. Long-term testing demonstrated high durability of $Ni/GDC–Al_2O_3$ at 650 °C with no detectable carbon deposition, consistent with thermodynamic equilibrium analysis.

Keywords: dry reforming of methane; Ni catalysts; Al_2O_3 support; GDC promoter

1. Introduction

The incentive to reduce the carbon footprint of power systems is driving the development and introduction of **low-carbon and zero-carbon fuels**. Hydrogen (H_2) is widely regarded as an energy carrier with significant potential for decarbonizing industrial processes [1]. H_2 can be produced via dry methane reforming (DRM), a process that simultaneously consumes methane (CH_4) and carbon dioxide (CO_2). This makes DRM an attractive route not only for H_2 production but also for the mitigation of greenhouse gas emissions, thereby contributing to environmental impact reduction. The overall chemical reaction of the DRM is as follows [2]:

$$CH_4 + CO_2 \rightleftharpoons 2H_2 + 2CO \qquad \Delta H_{@298} = +247\ \text{kJ/mol} \qquad (1)$$

The elevated temperatures are required to overcome the activation barrier of the reaction and achieve appreciable reaction rate. To facilitate the reaction, it is typically performed over suitable catalysts which provide an alternative reaction pathway with a lower effective activation energy [3]. However, catalyst performance is often severely compromised by carbon deposition, metal sintering, and insufficient long-term stability under the **demanding reaction conditions** required for DRM [4]. Consequently, the development of robust catalysts remains a critical research focus.

Noble metal catalysts such as ruthenium (Ru), rhodium (Rh), platinum (Pt), and palladium (Pd) have demonstrated excellent catalytic activity and resistance to carbon formation in DRM due to their superior ability to activate CH_4 and suppress coke formation [3]. Despite these advantages, their high cost and limited availability significantly restrict their large-scale industrial application. In contrast, nickel (Ni) catalysts have emerged as a promising alternative owing to their high activity for CH_4

 doi:10.20944/preprints202602.1593.v1

activation, abundance, and economic viability. Nevertheless, Ni catalysts are susceptible to sintering and carbon deposition, which leads to rapid deactivation [5].

In Ni-based catalysts, the catalyst support plays a key role in determining Ni species dispersion, thermal stability, and resistance to deactivation [4]. Therefore, careful choice of support is an important design parameter for improving the performance and durability of Ni catalysts. Common supports for Ni-based systems include metal oxides such as alumina (Al_2O_3), magnesia (MgO), ceria (CeO_2), and lanthana (La_2O_3) [6].

Within the group of oxide supports, Al_2O_3 has emerged as one of the most widely used materials due to its high surface area, excellent thermal stability, mechanical strength, and favorable interaction with Ni species [7]. Despite these advantages, the Ni/Al_2O_3 catalysts still face challenges related to coke formation and limited oxygen mobility, necessitating further modification [8].

To improve the performance and stability of the Ni/Al_2O_3 catalysts, the introduction of suitable promoters has been widely investigated. Promoters can modify the surface, enhance Ni dispersion, increase oxygen mobility, and facilitate the removal of carbonaceous species formed during DRM [2]. Numerous studies have reported that the incorporation of CeO_2 into Ni/Al_2O_3 catalysts as a promoter significantly enhances catalytic performance during DRM [9-13].

To further optimize catalytic activity, CeO_2 can be doped with gadolinium (Gd), forming Gd-doped ceria (GDC). While several studies have investigated GDC as a support or promoter for Ni-based catalysts in DRM [14-20], few studies, to the authors' knowledge, have examined DRM over Ni/GDC–Al_2O_3 catalysts. G.X. Zhang et al. [21] investigated the effects of Gd doping on the structure and DRM activity of Gd-promoted Ni/CeO_2–Al_2O_3 catalysts with different Gd_2O_3 loadings and examined their DRM performance in a fixed-bed quartz reactor at 500–800 °C. Their study demonstrated that calcination at 800 °C significantly influenced catalytic performance, while Gd addition notably enhanced both reaction activity and resistance to carbon deposition. Among the catalysts tested, Ni/CeO_2–Al_2O_3 with 1.2 wt% Gd_2O_3 exhibited the highest catalytic activity and stability. Y. Khani et al. [22] evaluated a series of Ni-based catalysts for CH_4 reforming using reactors coated with Ni/X–Al_2O_3 (X = Ce, Zr, Gd) and Ni/$CeZr_{0.5}GdO_4$ catalysts over the temperature range of 500–800 °C, and demonstrated that the Ni/Ce–Zr–Gd–Al_2O_3 catalyst exhibited appreciable CH_4 conversion and reasonable stability under reaction conditions confirming the beneficial role of combined Ce–Zr–Gd promotion in enhancing Ni/Al_2O_3 catalytic performance.

The present study aims to experimentally investigate the performance of Ni/Al_2O_3 and Ni/GDC–Al_2O_3 catalysts in DRM using a fixed-bed quartz reactor under various operating conditions. The effects of operating temperature, gas mixture residence time in the reactor, and catalyst type on reforming performance are evaluated. The experimental results are further compared with thermodynamic equilibrium calculations to identify the operating conditions under which the reforming behavior most closely approaches equilibrium while ensuring minimal carbon deposition, thereby promoting catalyst stability.

2. Experimental Setup

The dry reforming experiments were conducted using the setup shown schematically in Fig. 1. A premixed gas stream consisting of CH_4, CO_2, and nitrogen (N_2) was introduced into the reformer, which was positioned inside a horizontal Carbolite furnace (2 kW maximum power, maximum temperature 1200 °C). The furnace comprised a ceramic tube (650 mm length, 65 mm inner diameter), within which a centered tubular quartz reactor (10 mm inner diameter, 12 mm outer diameter, 900 mm length) was placed. Axial temperature measurements using a type K thermocouple indicated that the temperature distribution along the quartz tube is almost uniform, with a temperature deviation of less than 5 °C.

For the experiments, two types of catalyst beds were prepared by mechanical mixing. One contained 0.4 g of commercial NiO powder, characterized by a BET surface area of 3.5 $m^2 \cdot g^{-1}$ supplied by Fuel Cell Materials Inc. [23], mixed with 3.0 g of porous Al_2O_3 microspheres supplied by MaTecK Inc. [24]. The other contained 0.4 g of a NiO–GDC composite (60 wt% NiO – 40 wt% $Gd_{0.1}Ce_{0.9}O_{2-x}$), with a BET surface area of 4 $m^2 \cdot g^{-1}$ supplied by Fuel Cell Materials, mixed with 3.0 g of porous porous Al_2O_3 microspheres. The catalyst bed (40 mm in length) was positioned at the center of the furnace to

 doi:10.20944/preprints202602.1593.v1

ensure isothermal operation. Prior to each experiment, the catalysts were reduced in situ under H_2 flow.

The total flow rate of the gas mixture is controlled using a Bronkhorst mass flow controller and set to either 500 ml/min or 2000 ml/min, corresponding to residence times of approximately 0.4 s and 0.1 s within the reformer, respectively. The gas stream exiting the reformer is directed to a Aglient 490 Micro gas chromatograph (GC) for measuring the mole fractions of H_2, carbon monoxide (CO), CH_4, N_2 and CO_2, with an estimated relative uncertainty of 2%. Prior to entering the GC, water (H_2O) vapor is removed using a silica gel dryer to prevent moisture interference, as the instrument is highly sensitive to H_2O and can be damaged by exposure. The GC exhaust stream is discharged to the chimney. Both the GC and the mass flow controllers are operated and monitored through a computer based control system.

The feed composition consists of 2% CH_4, 4% CO_2, and 94% N_2. For this gas mixture, the chemical transformation governed by Eq. 1 can be presented as:

$$0.02\ CH_4 + 0.04\ CO_2 + 0.94\ N_2 \rightarrow 0.04\ H_2 + 0.04\ CO + 0.02\ CO_2 + 0.94\ N_2 \quad (2)$$

The low fractions of CH_4 and CO_2 are selected because, as mentioned above, the dry reforming reaction is highly endothermic, and limiting the reactant fractions lowers the overall heat demand of the system. This minimizes temperature gradients within the reactor and thereby helps maintain a uniform temperature distribution, which is essential for reliable kinetic measurements. Furthermore, a CO_2/CH_4 ratio of 2, which is above the stoichiometric value (Eq.1), decreases the tendency for carbon deposition because CO_2 can supply oxygen species that help gasify carbon formed from CH_4 and CO cracking [25]. This effect is supported by equilibrium calculations, which indicate that excess CO_2 suppresses carbon deposition. In this study, the equilibrium calculations were performed using a computational program based on the Gibbs free-energy minimization method [26]. Equilibrium calculations accounted for 53 common gas species in C-H-O system [27], along with condensed H_2O and carbon. Following equilibrium determination, species fractions were recalculated by removing H_2O from the gas mixture and re-normalizing the remaining components to enable comparison with the GC measurements.

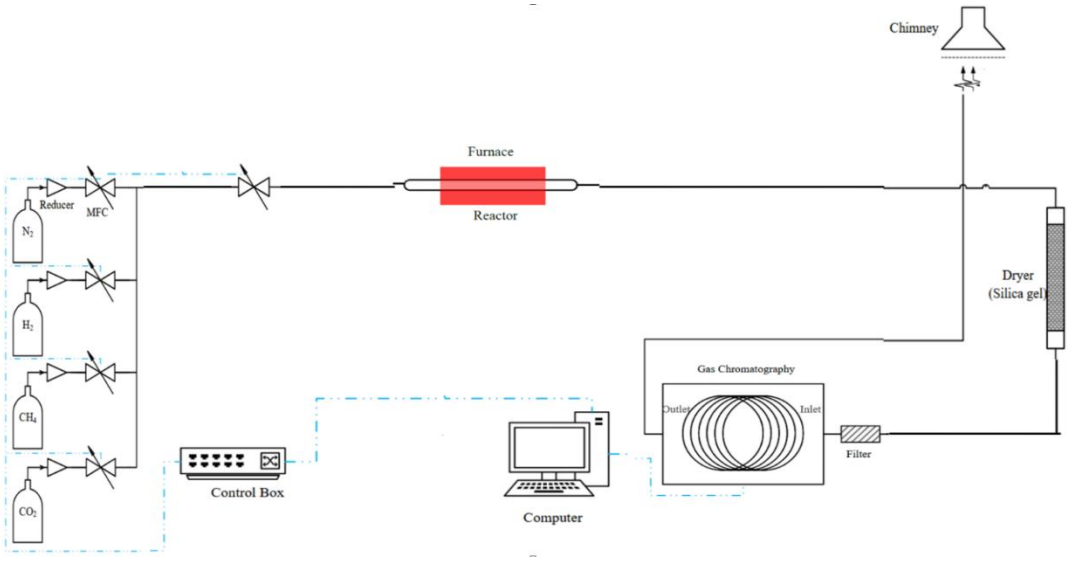

Figure 1. Schematic of the experimental setup.

3. Results and Discussion

Figures 2a and 2b show the CH_4 and CO_2 mole fractions, respectively, measured over the reactor temperature interval of 400–800 °C at residence times of 0.1 s and 0.4 s using Ni/Al_2O_3 and Ni/GDC–Al_2O_3 catalysts, alongside thermodynamic equilibrium mole fractions calculated for comparison. As shown in Fig. 2a, the CH_4 fraction at 400 °C is approximately 2% for both catalysts and residence times, corresponding to the CH_4 inlet concentration before any reforming occurs. With increasing

 doi:10.20944/preprints202602.1593.v1

temperature, the CH_4 fraction decreases, reflecting enhanced reforming activity and a trend toward the equilibrium concentration. At 600 °C over the Ni/Al_2O_3 catalyst, roughly 20% of the CH_4 is converted at the residence time of 0.1 s, whereas approximately 60% is converted at 0.4 s, demonstrating the substantial influence of residence time on the extent of CH_4 reforming. The results also indicate that at 750 °C, the CH_4 concentration is reduced to below 0.1% at a residence time of 0.4 s while at 0.1 s, approximately 75% of the CH_4 is reformed.

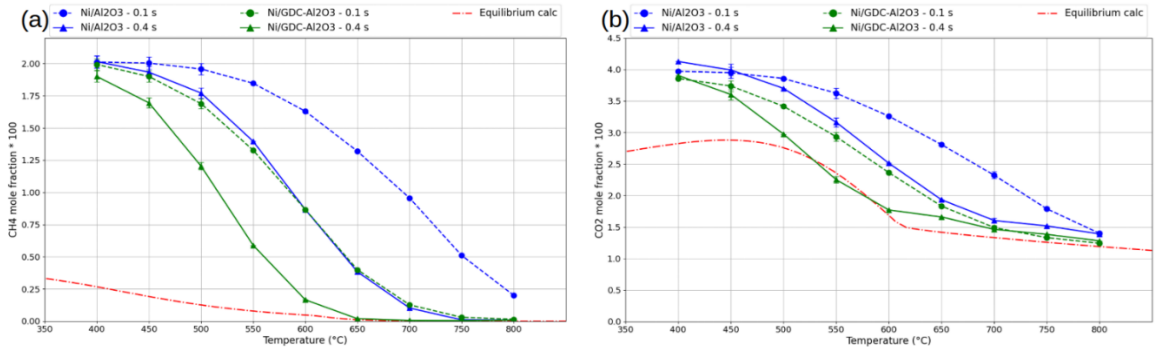

Figure 2. Experimental and equilibrium mole fractions as functions of temperature over Ni/Al_2O_3 and $Ni/GDC–Al_2O_3$ catalysts at residence times of 0.1 s and 0.4 s: (a) CH_4 and (b) CO_2.

A similar trend is observed for the experiments conducted with the $Ni/GDC\text{-}Al_2O_3$ catalyst. Comparison of the two catalysts indicates that the reforming process proceeds more rapidly with $Ni/GDC\text{-}Al_2O_3$. For instance, at 600 °C and a residence time of 0.1 s, approximately 60% of the CH_4 is reformed, which is comparable to the conversion achieved with Ni/Al_2O_3 at the same temperature but at a longer residence time of 0.4 s. As shown, near-total CH_4 conversion at a residence time of 0.4 s is achieved at 650 °C, representing an approximately 100 °C decrease in the temperature required compared with the Ni/Al_2O_3 catalyst under the same residence time.

The CO_2 variations exhibit behavior similar to that of CH_4, as shown in Fig. 2b. This fraction at 400 °C is approximately 4% for both catalysts and residence times, corresponding to the CO_2 inlet concentration. With increasing temperature, the CO_2 fraction decreases, reflecting enhanced reforming activity and a trend toward the equilibrium fraction of about 1.5%. The effects of residence time and catalysts on CO_2 conversion are similar to those observed for CH_4. For instance, at 600 °C over the Ni/Al_2O_3 catalyst, roughly 20% of the CO_2 is converted at a residence time of 0.1 s, whereas approximately 40% is converted at 0.4 s which is comparable to the value achieved with $Ni/GDC\text{-}Al_2O_3$ at the same temperature but with a shorter residence time of 0.1 s.

Figures 3a and 3b present the H_2 and CO mole fractions, respectively, as functions of reactor temperature at residence times of 0.1 s and 0.4 s, measured using Ni/Al_2O_3 and $Ni/GDC–Al_2O_3$ catalysts, together with comparisons to equilibrium calculations. As shown in Fig. 3a, for both catalysts and residence times, the H_2 fraction at 400 °C is zero before reforming occurs, and then increases with temperature, in agreement with the CH_4 reforming trends in Fig. 2a. At 600 °C over the Ni/Al_2O_3 catalyst, the H_2 fraction is 1.7% for a residence time of 0.4 s and about 0.5% for 0.1 s, demonstrating the effect of residence time. At 750 °C, the H_2 fraction reaches about 3% at 0.4 s, approaching the equilibrium H_2 fraction, whereas a lower value of 2.4% is observed at 0.1 s. Experiments using the $Ni/GDC–Al_2O_3$ catalyst exhibit a similar trend, with accelerated H_2 production. For example, the H_2 fraction tends toward its equilibrium value at about 650 °C with the $Ni/GDC\text{-}Al_2O_3$ catalyst at a residence time of 0.4 s, which is about 100 °C lower than the temperature required under identical residence time conditions when using the Ni/Al_2O_3 catalyst.

 doi:10.20944/preprints202602.1593.v1

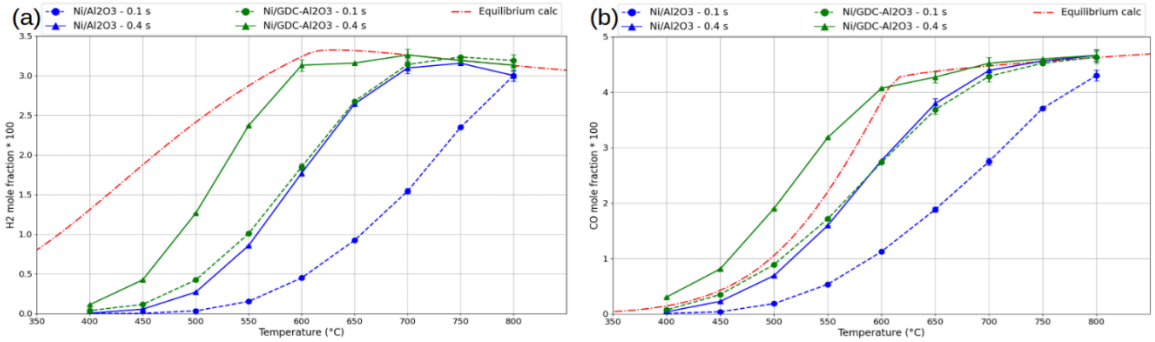

Figure 3. Experimental and equilibrium mole fractions as functions of temperature over Ni/Al_2O_3 and $Ni/GDC–Al_2O_3$ catalysts at residence times of 0.1 s and 0.4 s: (a) H_2 and (b) CO. .

The CO variations exhibit behavior similar to that of H_2, as shown in Fig. 3b. At 400 °C, the fraction is zero before reforming occurs and then increases with temperature. At 650 °C over the Ni/Al_2O_3 catalyst, the CO fraction is about 3.8% at a residence time of 0.4 s, and at 750 °C it reaches 4.5%, approaching equilibrium. Experiments using the $Ni/GDC–Al_2O_3$ catalyst follow a similar trend, exhibiting accelerated CO production consistent with the faster CH_4 and CO_2 consumption observed in Fig. 2a and 2b. For instance, at 600 °C over the $Ni/GDC–Al_2O_3$ catalyst, the CO fraction is approximately 4% at a residence time of 0.4 s and about 2.8% at 0.1 s, where the latter is comparable to that obtained with Ni/Al_2O_3 at the same temperature and a residence time of 0.4 s.

Comparison of the measured mole fraction values, which are close to equilibrium (Figures 2 and 3), with those derived by Eq. 2 reveals clear differences. The measured fractions of H_2, CO_2, and CO are about 3%, 1.5%, and 4.5%, respectively, whereas Eq. 2 indicates approximately 4%, 2%, and 4%. These discrepancies show that Eq. 2 alone cannot fully describe the DRM chemical reaction system.

We attribute the discrepancies to H_2O formation. Usually this process is described by the endothermic reverse water–gas shift (RWGS) reaction (Eq. 3 [2]), which consumes H_2 and CO_2 and produces CO and H_2O, thereby decreasing the H_2 and CO_2 mole fractions while increasing the CO mole fraction in the product relative to those derived by Eq. 2.

$$CO_2 + H_2 \rightleftharpoons CO + H_2O \qquad \Delta H_{@298} = +41 \text{ kJ/mol} \qquad (3)$$

Furthermore, at some measurement points, carbon deposition was observed, as indicated by changes in catalyst color and reactor pressure. The formation of solid carbon cannot be explained by Eq. 2 or Eq. 3. Commonly it is attributed to the Boudouard reaction (Eq. 4 [2]).

$$2CO \rightleftharpoons CO_2 + C_s \qquad \Delta H_{@298} = -247 \text{ kJ/mol} \qquad (4)$$

where C_s is solid carbon. This reaction is strongly exothermic, and C_s forms from CO as the reaction proceeds. Increasing the temperature, however, promotes the endothermic reverse reaction, which gasifies C_s and forms CO. However, it should be pointed out that CH_4 reforming is a multi-step complex process and additional reactions might be added to the reaction mechanism to describe it properly.

The formation of H_2O and solid carbon is also shown by the equilibrium calculations. Figure 4 presents the equilibrium fractions of H_2O and solid carbon as functions of temperature. Under conditions where the experimental measurements tend to equilibrium (Figures 1 and 2), the H_2O mole fraction is approximately 0.5% and increases slightly with temperature.

 doi:10.20944/preprints202602.1593.v1

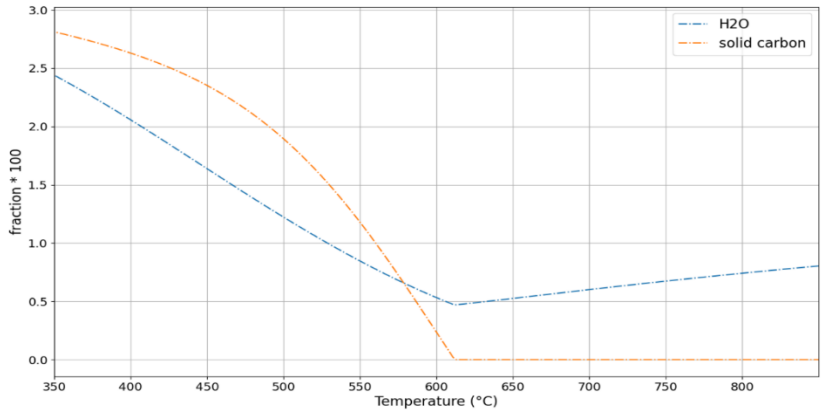

Figure 4. Equilibrium fractions of H_2O and solid carbon as functions of temperature.

The equilibrium calculation **implies** a carbon deposition of approximately 2% at 400 °C. As the temperature increases, the solid carbon fraction decreases to zero above 620 °C. This thermodynamic trend also qualitatively aligns with our experimental observations, as carbon deposition on the Ni/GDC–Al_2O_3 catalyst was observed within a few hours during reforming at 550 °C, whereas at 650 °C no carbon deposition **was** recognized, and the process proceeded stably for more than one week, indicating effective suppression of solid carbon formation at elevated **temperatures**.

4. Conclusions

This study investigated the catalytic performance of Ni/Al_2O_3 and Ni/GDC–Al_2O_3 for DRM process within a fixed-bed tubular reactor across a temperature range of 400–800 °C at gas mixture residence times of 0.1 s and 0.4 s. The results show that higher reactor temperatures and longer gas residence times noticeably increase CH_4 and CO_2 consumption, as well as H_2 and CO production rates. Notably, integrating GDC promoter into the Al_2O_3 support substantially accelerates reforming kinetics. This catalytic enhancement is evidenced by the fact that Ni/GDC–Al_2O_3 at a residence time of 0.1 s achieves CH_4 and CO_2 conversion efficiencies, as well as H_2 and CO yields, comparable to those of Ni/Al_2O_3 at 0.4 s. The superior kinetics of the Ni/GDC–Al_2O_3 catalyst are further evidenced at a 0.4 s residence time, where complete CH_4 and about 60% CO_2 conversion is reached at about 650°C, which is approximately 100°C lower than the temperature required by the Ni/Al_2O_3 catalyst.

A comparison of the measured mole fraction values, which are approaching equilibrium (temperatures above 650 °C) with those derived by the single DRM reaction reveals a clear discrepancy, indicating that the DRM reaction alone is insufficient to describe the DRM chemical process. This discrepancy is attributed to H_2O production, which is usually described by the RWGS reaction. Additionally, carbon deposition observed at low temperatures, commonly attributed to the Boudouard reaction, suggests that it should also be considered when describing the DRM system. Long-term testing confirmed the high durability of the Ni/GDC-Al_2O_3 catalyst, with no carbon deposition detected at 650 °C, consistent with zero solid carbon equilibrium calculation.

Overall, the results demonstrate that Ni/GDC–Al_2O_3 is a highly active catalyst for the DRM process, offering enhanced reforming kinetics and good durability at temperatures above 600 °C, making it a promising candidate for efficient syngas production under moderate operating conditions.

Informed Consent Statement: Informed consent was obtained from all subjects involved in the study.

Acknowledgments: The authors would like to express their thanks to the China Scholarship Council (CSC), Dutch Research Council (NWO), and Clean Energy Transition Partnership Program (CETP) for financial support, and M. Bosker and T. H. B. Langedijk from the University of Groningen, The Netherlands.

Conflicts of Interest: The authors declare no conflicts of interest.

References

 doi:10.20944/preprints202602.1593.v1

1. **Y. Zhu, G. A. Keoleian, D. R. Cooper,** *"The role of hydrogen in decarbonizing U.S. industry: A review"*, Renewable and Sustainable Energy Reviews, **214** (2025) 115392.
2. D. W. Green and M. Z. Southard, *"Perry's Chemical Engineers' Handbook"*, 9th ed., McGraw-Hill Education, New York, 2018.
3. D. Pakhare and J. Spivey, "A review of dry (CO_2) reforming of methane over noble metal catalysts" *Chem. Soc. Rev.* , 43 (2014) 7813–7837.
4. J. You, L. Lai, Y. Chen, *"Recent Advances in Strong Metal-Support Interaction Engineering for Dry Reforming of Methane Catalysts"*, Wiley, 2025.
5. H. O. Seo, *"Recent Scientific Progress on Developing Supported Ni Catalysts for Dry (CO_2) Reforming of Methane"*, **Catalysts**, *8 (2018)* 110.
6. E. Meloni, M. Martino, and V. Palma, *"A Short Review on Ni Based Catalysts and Related Engineering Issues for Methane Steam Reforming*", Catalysts, 10 (2020) 352.
7. Y. Xu, X.h. Du, J. Li, P. Wang, J. Zhu, F.j. Ge, J. Zhou, M. Song, W.y. Zhu, *"A comparison of Al_2O_3 and SiO_2 supported Ni-based catalysts in their performance for the dry reforming of methane"*, **Fuel Process. Technol.**, 47 (2019) 199–208.
8. X. Gao, Z. Ge, G. Zhu, Z. Wang, J. Ashok, S. Kawi, *"Anti-Coking and Anti-Sintering Ni/Al_2O_3 Catalysts in the Dry Reforming of Methane: Recent Progress and Prospects"*, **Catalysts**, *11* (2021), 1003.
9. S. Aghamohammadi, M. Haghighi, M. Maleki, N. Rahemi, *"Sequential impregnation vs. sol–gel synthesized Ni/Al_2O_3–CeO_2 nanocatalyst for dry reforming of methane: Effect of synthesis method and support promotion"*, **J. Mol. Catal. Chem.** , *431*(**2017**) 39–48.
10. J. Han, Y. Zhan, J. Street, F. To, F. Yu, *"Natural gas reforming of carbon dioxide for syngas over Ni–Ce–Al catalysts"*, **Int. J. Hydrogen Energy.,** 29 (2017) 18364–18374.
11. N. Laosiripojana, W. Sutthisripok, and S. Assabumrungrat, *"Synthesis gas production from dry reforming of methane over CeO2 doped Ni/Al2O3: Influence of the doping ceria on the resistance toward carbon formation"*, **Chem. Eng. J.** , 112 (2005) 13-22.
12. R. Babakouhi, S.M. Alavi, M. Rezaei, F. Jokar, M. Varbar, and E. Akbari, *"Hydrogen production through combined dry reforming and partial oxidation of methane over the Ni/Al2O3–CeO2 catalysts*", **Int. J. Hydrogen Energy.**, 60 (2024) 2024.
13. A.L.A. Marinho, F.S. Toniolo, F.B. Noronha, F. Epron, D. Duprez, and N. Bion, *"Highly active and stable Ni dispersed on mesoporous CeO2–Al2O3 catalysts for production of syngas by dry reforming of methane*", Appl. Catal. B Environ. , 281 (2021) 119459.
14. **E. Ioannidou, S. G. Neophytides, and D. K. Niakolas,** *"Au-Mo-Fe-Ni/CeO_2(Gd_2O_3) As Potential Fuel Electrodes For Internal CO_2 Reforming of CH_4 in Single SOFCs"*, **ECST,** 111 (2023) 2473–2485.
15. H.R. Gurav, S. Dama, V. Samuel, and S. Chilukuri, *"Influence of preparation method on activity and stability of Ni catalysts supported on Gd doped ceria in dry reforming of methane*", **J. CO2 Util.** , 20 (2017) 357-367.
16. I. Unal, S. Meisuria, M. Choolaei, T.R. Reina, and B.A. Horri, *"Synthesis and characteristics of nanocrystalline Ni1−xCoxO/GDC powder as a methane reforming catalyst for SOFCs*", Ceram. Int. , 44 (2018) 6851-6860.
17. W. Wang, S.P. Jiang, A.L.Y. Tok, and L. Luo, *"GDC-impregnated Ni anodes for direct utilization of methane in solid oxide fuel cells*", J. Power Sources, 159 (2006) 68-72.
18. H.R. Gurav, S. Dama, V. Samuel, and S. Chilukuri, *"Influence of preparation method on activity and stability of Ni catalysts supported on Gd doped ceria in dry reforming of methane*", J. CO2 Util., 20 (2017) 357-367.
19. A.L.A. Marinho, R.C. Rabelo-Neto, F. Epron, F.S. Toniolo, F.B. Noronha, and N. Bion, *"Effect of Metal Dopant on the Performance of Ni@CeMeO2 Embedded Catalysts (Me = Gd, Sm and Zr) for Dry Reforming of Methane*", Methane, 1 (2022) 300-319.
20. A.S. AlFatesh, *"Promotional effect of Gd over Ni/Y2O3 catalyst used in dry reforming of CH4 for H2 production*", **Int. J. Hydrogen Energy**, 42 (2017) 18805-18816.
21. G.X. Zhang, Y. Wang, X.K. Li, Y.K. Bai, L. Zheng, L. Wu, and X.L. Han, *"Effect of Gd promoter on the structure and catalytic performance of mesoporous Ni/Al2O3-CeO2 in dry reforming of methane*", Ind. Eng. Chem. Res. , 2018.

 doi:10.20944/preprints202602.1593.v1

22. Y. Khani, F. Bahadoran, Z. Shariatinia, M. Varmazyari, and N. Safari, "*Synthesis of highly efficient and stable Ni/CexZr1−xGdxO4 and Ni/X−Al2O3 (X = Ce, Zr, Gd, Ce-Zr-Gd) nanocatalysts applied in methane reforming reactions*", Ceram. Int. , 46 (2020) 25122-25135.
23. Fuel Cell Materials, Inc., USA, https://www.fuelcellmaterials.com
24. MaTecK GmbH, Germany, https://www.mateck.com
25. A. G. S. Hussien and K. Polychronopoulou, "*A Review on the Different Aspects and Challenges of the Dry Reforming of Methane (DRM) Reaction*", **J. Nanomater.** , 12 (2022) 3400.
26. K. K. Kuo, Principles of Combustion, John Wiley and Sons, 2005.
27. G. P. Smith, D. M. Golden, M. Frenklach, N. W. Moriarty, B. Eiteneer, M. Goldenberg, GRI-Mech 3.0, 2000, http://combustion.berkeley.edu/gri-mech